Journal of *Marine Science and Engineering*

MDPI

Article

Beachrock as a Natural Coastal Resource in Antiquity: Evidence from Southern Israel

Amir Bar [1,2,*], Elie Haddad [3], Yotam Asscher [4,5], Ehud Galili [6,7], Revital Bookman [2] and Dov Zviely [8]

[1] Central District, Central Regional Office, Israel Antiquities Authority, Jerusalem 9100402, Israel
[2] Department of Marine Geosciences, The Leon H. Charney School for Marine Sciences, University of Haifa, Haifa 3498838, Israel; rbookman@univ.haifa.ac.il
[3] Mega Projects Department, Israel Antiquities Authority, POB 586, Jerusalem 91004, Israel; haddad@israntique.org.il
[4] Department of Culture Heritage, School of Archaeology and Maritime Cultures, University of Haifa, Haifa 3498838, Israel; yotama@israntique.org.il
[5] Artifacts Treatment and Conservation Department, Israel Antiquities Authority, Jerusalem 9100402, Israel
[6] The Zinman Institute of Archaeology, University of Haifa, Haifa 3498838, Israel; galiliudi@gmail.com
[7] The Recanati Institute for Maritime Studies, University of Haifa, Haifa 3498838, Israel
[8] Faculty of Marine Sciences, Ruppin Academic Center, Emek-Hefer 40250, Israel; dovz@ruppin.ac.il
* Correspondence: amirb@israntique.org.il

Abstract: Beachrock is a sedimentary rock that forms rapidly through the cementation of beach-associated clasts by calcium carbonate within the intertidal zone. On the southern coast of Israel, Holocene beachrock exposures typically appear as linear, shore-parallel platforms that dip seawards. In the archeological record, beachrock was exploited as a natural resource for various purposes, including the production of querns, millstones, basins, building stones, and other architectural elements. At Tel Yavne, a site continuously settled from the Chalcolithic period to the present day, excavations in the eastern and southern fringes revealed an extensive industrial compound dating to the Byzantine and early Islamic periods. This compound underscores the settlement's economic and industrial prominence during those eras. Numerous beachrock artifacts were uncovered, and this study examines their practical applications while characterizing their composition and microstructure. This research highlights the role of beachrock as a key resource, providing insights into inland–coastal economic interactions in antiquity and broadening our understanding of its use within the socio-economic landscape of the region.

Keywords: beachrock; coastal archaeology; paleogeography; natural resource; raw material; stone finds

check for updates

Academic Editor: Niki Evelpidou

Received: 29 December 2024
Revised: 15 January 2025
Accepted: 22 January 2025
Published: 26 January 2025

Citation: Bar, A.; Haddad, E.; Asscher, Y.; Galili, E.; Bookman, R.; Zviely, D. Beachrock as a Natural Coastal Resource in Antiquity: Evidence from Southern Israel. *J. Mar. Sci. Eng.* **2025**, *13*, 240. https://doi.org/10.3390/jmse13020240

Copyright: © 2025 by the authors. Licensee MDPI, Basel, Switzerland. This article is an open access article distributed under the terms and conditions of the Creative Commons Attribution (CC BY) license (https://creativecommons.org/licenses/by/4.0/).

1. Introduction

1.1. Definition of Beachrock

The term beachrock (hereafter BR) refers to coastal sedimentary rock found in the intertidal zone, composed of beach-related clasts consolidated by calcium carbonate cements [1]. Most BR formations occur on sandy beaches with micro-mesotidal ranges, predominantly in tropical and subtropical climates. Key regions for BR studies include the Mediterranean, Caribbean, and Atlantic coasts and the atolls of the Pacific and Indian Oceans [2].

Most BR studies focus on seaward-dipping formations [3], typically outcropping parallel to the shore as longitudinal ridges and exhibiting a distinct morphology of flat platforms dipping seaward at a similar gradient as the beach face. Beachrock outcrops are a prominent feature of many beaches, making them an ideal subject for paleo-geographic studies.

These include shoreline migration and sea-level fluctuation assessments, particularly in the eastern Mediterranean during the later part of the Holocene [3–10].

Beachrock forms at the subsurface over a timescale as short as a few years, with its initial consolidation influenced strongly by microbiological activity. The clastic components of BR correspond to the unconsolidated sediment found on the beach where it forms. [3,5,9]. The environmental conditions necessary for BR consolidation at the sea–land interface include biogenic carbon sources, warm temperatures, high porosity, and significant sand accumulation. No single physio-chemical process has been definitively identified as the dominant global mechanism for BR formation. Instead, it appears to result from the interplay of multiple factors [5,11–13].

Beachrock is exposed when the overlying unconsolidated sediment is eroded by wave activity and local morphodynamics. Following exposure, waves can dislodge sections of BR, moving them from their original location and depositing them tens of meters inland [14–16].

1.2. Regional Setting

The Mediterranean coast of Israel extends 195 km and is divided into four sections: the southern coast (Figure 1), central coast, Carmel and Haifa Bay coasts, and western Galilee coasts. The Southern coast is characterized primarily by sandy beaches (typically up to 50 m wide) and coastal escarpments (up to 20 m high) formed by erosion of the coastal kurkar ridge. Beach sediments consist of clasts sourced from regional and local provinces, including quartz sand transported by longshore currents from the Nile River system. Aeolianite fragments, ranging from sand to pebble size, originate from erosion of the coastal ridge. Biogenic sand (shells and other skeletal and biogenic concretions remains) from coastal and shallow continental shelf environments are deposited by wave action [17–19].

The Mediterranean coastline of Israel features abundant BR outcrops (Figure 1c), appearing as strips up to ~1 m thick, and are typically flat platforms dipping westward in a stair-like arrangement [16,20,21]. The main cements in BR include magnesium-bearing calcite (>8 mole % $MgCO_3$) and aragonite [10,22–25].

Dating BR can involve radiocarbon analysis of shells or optically stimulated luminescence (OSL) dating of quartz grains [2]. OSL dating represents the beginning of diagenesis, occurring with the deposition of beach sediments. For example, OSL ages from BR samples on the central coast of Israel range from 2000 to 800 years BP (before present) [10,26,27]. In cases where ceramics are embedded in BR beds, *terminus post quem* dating can be established by dating pottery. Archaeological materials, including pottery sherds and marble fragments, have been found embedded in BR outcrops at sites such as Akko, Dor, Caesarea, Palmachim, and Ashkelon [21]. At Atlit Bay, near the Crusader cemetery and south of the Oren River outlet, ceramic vessels from the Iron Age (2700–2800 years BP) were found embedded in BR [28]. At Akko, pottery dated to the Persian period (2333–2586 years BP) was documented [29].

Most BR along Israel's coastline formed in the upper Holocene and are considered geologically young [10,21,26,27], contrasting with Upper Pleistocene beach deposits (BDs) from the last interglacial maximum (MIS 5e, ~134–116 ka BP). These earlier deposits have been identified and documented as sea-level indicators along the Carmel and Galilee coasts and are similar to formations that have been observed across the Mediterranean [30,31].

Beachrock formation and exposure are influenced by coastal erosion during the last 4000 years caused by waves, currents, and storms and by minor sea-level fluctuations (~1 m). Sand quarrying and BR extraction, particularly in the last century before the enactment of the "Zifzif Law" in 1963 [32], have also significantly impacted the state of BR exposures [32,33]. Once exposed, BR is subject to physical forces that erode and

separate plates from the bed. These plates accumulate near the outcrop edges and in the backshore [16].



Figure 1. Location map: (**a**) The eastern Mediterranean region (background map: Terrain Light background layer by EOX—4326). (**b**) The southern coastline of Israel with studied sites marked. Sampling locations of natural intertidal BR exposures are marked with orange dots; the location of the excavation site, where artifacts made of beachrock were sampled, are marked with a yellow dot. (background map: Sentinel-2 Cloudless layer for 2016 by EOX—4326). (**c**) Typical appearance of beachrock outcrops along the southern Mediterranean coast of Israel, with an example of BR blocks accumulation at the waterfront, from Ashdod, view to the north.

Previous studies of BR outcrops along the Mediterranean coast of Israel have predominantly focused on the mineralogy and geochemical composition of Holocene and Pleistocene sediments [22,24] or their role in coastal cliff retreat during the Holocene (e.g., [26,27]). In archaeological contexts, the most common use of BR was in the creation and design of abrasive tools such as querns and millstones. Spatial pattern analyses of stone tools, reported from surveys and excavations dated to the 7th–11th centuries CE, reveal that rotary querns were very common. These tools are flat, round (0.25–0.45 m wide), and made of natural rocks, preferably basalt or BR [34]. Querns made from natural rocks were used to grind grains into flour, press fruits for oil, and crush soft materials like ceramics. The use of millstones across the Mediterranean is very common from the Roman

era to modern times. Smaller millstones (0.25–0.92 m) were operated manually, while larger stones (more than 0.45 m) required animal, hydraulic, or wind power [29,35,36].

BR querns and grindstones have been discovered at numerous sites along Israel's coast [37–42]. Yoram Neri [43] studied saddle-quern-type milestones made of BR found at over 30 sites, ranging from the Chalcolithic to Roman periods, across the coastal plain and northern Negev (from Achziv to Shiqmim). These querns shared typological similarities with those made of basalt, granite, and limestone. A significant negative correlation was noted between BR presence and distance from the sea, with a maximum inland occurrence at Tel Lachish (~30 km). Hardness and abrasion tests showed that while BR was weaker than basalt, it outperformed limestone in resisting abrasion [43].

A BR quarry for cylindrical millstones was documented at Akko. The site included tens of circular rock cuts, broken stones left in-situ, tunnels, and stairs [29]. The quarry exploited well-consolidated BR, with high levels of consolidation aiding the detachment of stones. Quarrying was likely conducted during low tides, with wooden wedges used to facilitate separation during high tides. Pottery embedded in the BR indicates quarrying in the post-Persian period [32]. A BR ballista ball, likely Hellenistic, was found at the Hospitaller Compound in Akko [44].

In an Early Islamic context (~1389–926 years BP), BR rotary querns were discovered in Ramla [45–47]. During the Crusader period (~765–926 years BP), BR querns of varying sizes were used in olive-oil production installations at Apollonia (Arsuf-Arsur) [48].

Architectural uses of BR have been documented at several sites, albeit in minor quantities. BR plates were used as tomb covers during the Byzantine period at Tel Baruch [49] and as paving in an Early Islamic factory site southeast of Ramla [46,47]. Architectural elements made of BR were found in Rehovot [50,51]. In Ashdod Yam, BR was used in the Ribbat's construction and as pavements for coastal wells during the Byzantine and Islamic periods [21,52,53]. At Akko, a tomb roofed with BR slabs was excavated near Kibbutz Gesher Ha-Ziv [54].

In other contexts, BR exploitation was minimal. At Tel Yavne Yam, no significant use of BR in construction was recorded [55,56]. In Caesarea, BR was rarely used in construction but was documented as material for millstones and ship ballast [57,58]. Salvage excavations at Ashkelon revealed negligible use of BR as construction material [59].

In some cases, Pleistocene beach deposit rocks (e.g., Yasaf Member) were exploited as an alternative to BR. For example, at the Hospitaller compound at Akko during the Crusader period [60], at the Ottoman aqueduct in Akko, and Chalcolithic olive processing installations at Hishuley Carmel that utilized MIS 5e deposits collected from nearby streams [61].

2. The Yavne East Excavation

Tel Yavne is located in the southern coastal plain of Israel (Figure 1), in the southeastern part of the city of Yavne. The site is situated on a ridge of calcareous cemented aeolianite sandstone (locally referred to as kurkar), approximately 7 km from the beach and about 0.3 km west of the Soreq River stream route. The tel covers an area of approximately 120,000 square meters, with its highest point reaching ~60 m above sea level [62] (and references within). Several excavations (mostly salvage) have been conducted around the tel over the past decade. These investigations indicate continuous settlement at the site from the Chalcolithic period to the present day, with peak activity occurring during the Byzantine period [63–71] (and references within).

This study was conducted as part of the first phase of the "mega" salvage excavation project at Yavne, carried out between 2019 and 2021 (Permit Numbers: A-8520; A-8656) under the direction of Elie Haddad, Liat Nadav-Ziv, and Jon Seligman. The excavations

focused on the eastern and southern fringes of the tel. Areas A and B, located approximately 400 m south of the tel (Figure 2), did not yield any BR finds. However, areas C1–C7, situated on the northeastern fringes of the tel, and areas G1–G8, located on its southeastern fringes, produced the majority of BR finds (Table 1). Area D, approximately 650 m southwest of areas A and B, was also excavated.

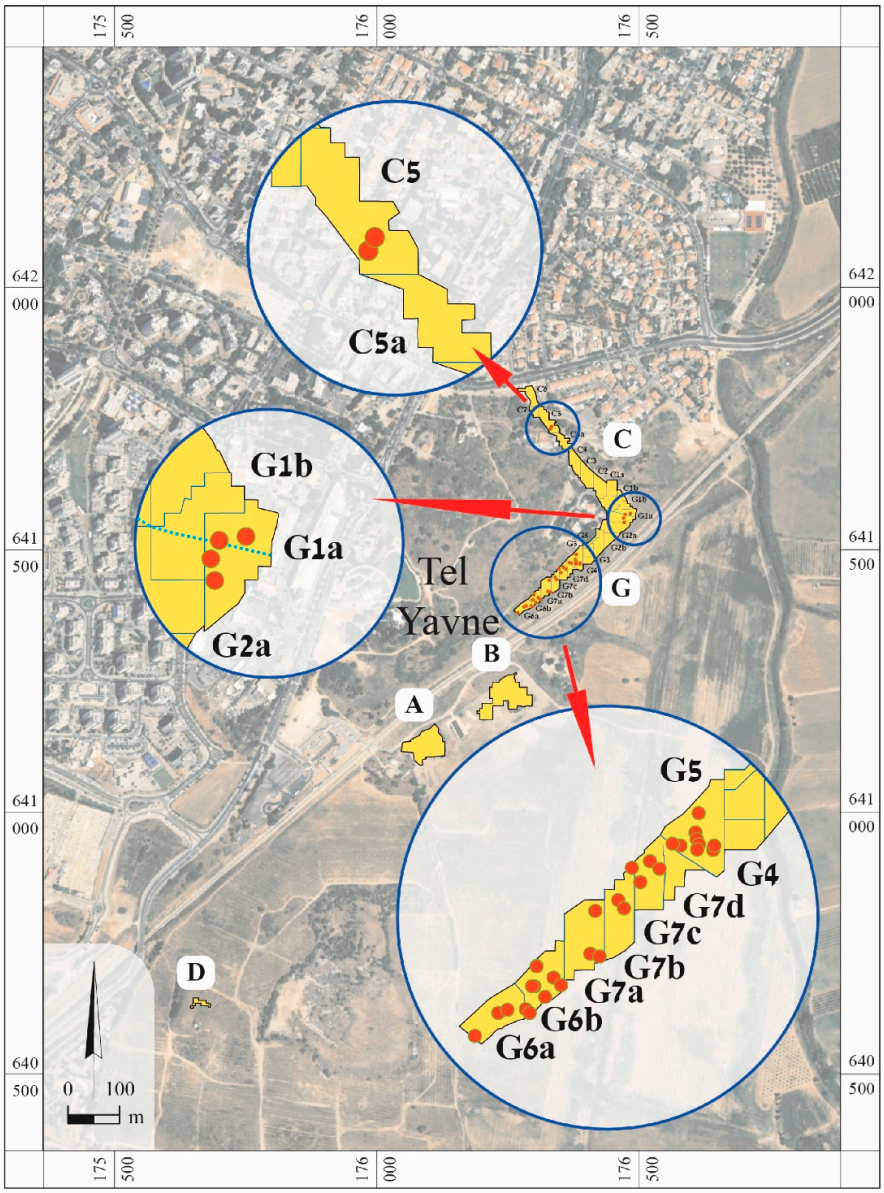

Figure 2. Tel Yavne and the location of the excavation areas. The locations where beachrock finds were discovered are marked with dots. The dotted blue line in the enlarged circle including the Area G1a and G2a section marks the location of the drainage tunnel remains (map: Y. Gumenny). Courtesy of the Israel Antiquities Authority (IAA).

In Area A, remains from the Chalcolithic, Late Iron, Persian, and Hellenistic periods were uncovered, though no BR finds were recorded. Area B and its vicinity revealed a large industrial compound dating to the Byzantine and Early Islamic periods. Excavations in Areas C and G uncovered a continuation of this industrial zone. The main findings in Area C include life-level remains, mosaic floors associated with the Byzantine wine industry, a deep drainage tunnel roofed in most parts with BR plates, and a street above it constructed with compacted fill composed of small ceramic fragments. Early Islamic

architectural remains, pottery kilns, and post-Early Islamic drainage tunnels were also documented, as well as houses that remained in use until 1948.

Table 1. Usage of beachrock in architecture and apparatuses in excavation areas C and G.

Serial Number	Excavation Area	Locus	Period	Archaeological Context
1	C5	24165	Byzantine	Pavement
2	C5	24264	Byzantine	Pavement
3	G1	30180	It has not yet been clarified	Pavement
4	G1	30120	NYD	Covering main tunnel
5	G1	30275	NYD	Covering excess tunnel
6	G1	42027	NYD	Pavement
7	G5	34582	Umayyad	Pavement
8	G5	34248	Umayyad	Inside a garbage pit
9	G5	34041	Ottoman	Pavement
10	G5	34116	Byzantine/Early Islamic	Pavement
11	G5	34248	Byzantine/Early Islamic	Pavement
12	G5	34041	Byzantine/Early Islamic	Pavement
13	G5	34066	Byzantine/Early Islamic	Pavement
14	G5	34116	Byzantine/Early Islamic	Pavement
15	G5	34240	Byzantine/Early Islamic	Pavement
16	G5	34396	Byzantine/Early Islamic	Pavement
17	G5	34303	Byzantine/Early Islamic	Part of apparatus
18	G5	34304	Byzantine/Early Islamic	Part of apparatus
19	G6a	35369	Byzantine/Early Islamic	Round millstone
20	G6a	35188	Umayyad	Roofing a water tunnel
21	G6a	35363	Late Byzantine	Pavement in room 4
22	G6a	35276	Umayyad	Pavement in room 5
23	G6b	35522	Ottoman	In a collapsed area
24	G6b	35529	Ottoman	In a collapsed area
25	G6b	35598	Ottoman	In a collapsed area
26	G6b	W35518	Ottoman	In a wall
27	G6b	W35582	Ottoman	In a wall
28	G6b	41070	Byzantine/Early Islamic	Roofing water tunnel
29	G6b	41321	Byzantine/Early Islamic	Pavement
30	G6b	41326	Byzantine/Early Islamic	Pavement
31	G7a	W39045	It has not yet been clarified	In a wall
32	G7a	W39019	Byzantine/Early Islamic	In a wall
33	G7b	36155	Byzantine/Early Islamic	Roofing a water tunnel
34	G7b	36030	Byzantine/Early Islamic	Roofing a water tunnel
35	G7b	36108	Byzantine/Early Islamic	Pavement
36	G7b	36125	Byzantine/Early Islamic	Pavement
37	G7c	37034	Umayyad	Pavement
38	G7c	37092	It has not yet been clarified	Pavement
39	G7c	37082	Byzantine/Early Islamic	Pavement
40	G7c	37092	Byzantine/Early Islamic	Pavement
41	G7c	37186	Byzantine/Early Islamic	Pavement
42	G7d	38005	Byzantine/Early Islamic	Round millstone

The periods in the table were determined based on the archeological context. Final dating is in progress. NYD—Not Yet Determined.

In Area D, an Ottoman-era watering tunnel was uncovered, reflecting agricultural activity around the tel during this period. These findings collectively suggest that a significant industrial complex surrounded the tel during the Byzantine and Early Islamic periods, indicating extensive human activity in those eras.

The excavations revealed a large assemblage of BR objects utilized for various purposes, including plates for roofing drainage tunnels, floor pavements, and walls in rooms and courtyards (for preliminary article in Hebrew, see [72]). Additional BR artifacts included working surfaces, plates with carved dimples, and grinding stones.

The extensive discovery of BR finds during the excavations prompted a multidisciplinary study encompassing documentation, data acquisition, sampling, and geoarchaeological analysis. This research aimed to determine whether BR was specifically chosen for certain applications due to its mechanical properties and to explore the connection between Yavne and the Mediterranean shoreline, reflecting the unique characteristics of this material.

This study examines the coastal orientation of Yavne by analyzing an assemblage of BR artifacts transported from the shoreline to the site through direct import and uncovered during excavation. The research addresses key questions, including the following: Why did the constructors of the industrial compound opt to use BR from the beach, despite the proximity of kurkar outcrops? When was the use of BR most prevalent? Was BR employed for specific purposes in a deliberate and planned manner? If so, what are the material properties of BR that offered advantages for those uses?

3. Materials and Methods

3.1. Systematic Field Observations

Identification of BR in the excavation areas involved examining plates covering drainage tunnels; documenting vessels, devices, and apparatuses made of BR; and analyzing their usage with 3D models. Samples were collected from in-situ BR outcrops at selected beaches (Figure 1) and from BR artifacts recovered at the site (Figure 2, Table 1).

Samples were taken from roofing plates of the main tunnel in Area G1 (L30120), including from a plate covering the split to the excess tunnel (L30275), and a rectangular BR slab found on the working surface, which was paved with mosaic, above the opening of the octagonal collecting vat in winepress 6 (Area G1), located approximately 20 m south of the tunnel.

Naturally exposed BR outcrops were examined in three sites at the southern coast of Israel (Figure 1). Samples were obtained from the upper surface of the Lingoid ridge (see [73]) and from block accumulation at the intertidal zone at four beaches: Tel Ashkelon (31.65757/34.53928), Ashdod (31.85254/34.66004), north of Tel Yavne Yam (31.92946/34.63829), and south of the current mouth of the Soreq River (Figure 1) near Kibutz Palmachim (31.93354/34.70221).

3.2. Texture and Mineralogical Composition Analysis

In the laboratory, micrographs were used to perform micro-morphological analysis of selected samples from both archaeological finds and in-situ BR outcrops. Fresh surfaces were prepared by polishing the samples, which were then examined under a stereoscope (Zeiss Stereo Discovery V12 and Zeiss Axioscope 5) and a digital microscope (Dino-Lite). The clastic composition and texture of specimens from Yavne were compared with thin sections representing BR outcrops along the southern Mediterranean coastline of Israel. This comparative analysis adhered to the principles outlined in visual comparators and estimation charts [74,75]. The samples were examined with an Olympus model microscope and a 3D digital microscope (HIROX RH-2000) equipped with high-intensity LED lighting.

Infrared spectroscopy (FTIR) was employed to provide mineral characterization of the samples obtained from Yavne. To create the infrared spectra, a gram of each sample was homogenized in an agate mortar, and approximately 0.2 mg was ground to a fine powder and then mixed with approximately 20 mg of KBr (FTIR grade). Samples were then pressed

into a 7 mm pellet using a hand press (PIKE Technologies). Infrared spectra were obtained using a Nicolet iS5 spectrometer at 4 cm^{-1} resolution. Results were compared to standard spectra available at the FTIR library of the Kimmel Center for Archaeological Science [76].

X-Ray diffraction (XRD) analysis was used to determine the mineralogical composition of chosen samples from both archaeological finds and BR outcrops. Bulk dry BR was gently crushed, sieved (2000µ and 1000µ), and powdered. Analysis was carried out using a Rigaku MiniFlex 600 benchtop XRD with a Cu source at 30 kV/10 mA from 3° to 70° at 0.05° increments by point detector. Mineral identification was carried out using the PDF2 database (International Centre for Diffraction Data), and mineralogical ratios were calculated using the relative intensity ratio method [77] with Rigaku PDXL software.

4. Results

4.1. Beachrock Finds and Context

The excavations in Areas C and G uncovered large-scale assemblages of BR objects used in various operational contexts (Table 1). Beachrock slabs served as a primary material for covering drainage tunnels at Yavne (Figure 3). The main tunnel, constructed along an east–west axis, extends approximately 58 m in length. It begins west of Area C1a and inclines eastward toward Area G1a, with the tunnel bottom at an elevation of 26.41 m above sea level in the west and 25.52 m above sea level in the east.



Figure 3. Beachrock architecture usage within the industrial compound at Tel Yavne. See Figure 2 for the locations of the excavation areas: (**a**) Beachrock slabs used in the main tunnel (samples location marked with dots, arrows mark the sections viewed in **b**,**c**) (photo: Peretz, A.). (**b**) Beachrock plate

(sample location marked with circle) covering the split section of the main drainage tunnel and the excess tunnel in Area G1. (**c**) Beachrock slabs arranged in a gable-like form, possibly serving as manholes or inspection entrances (photos: Elimelec, C.). Courtesy of the IAA.

The continuation of the tunnel eastward remains unclear. Portions of it were likely exposed during earlier excavations, including those by Sion [63] and Yannai [65].

4.1.1. The Tunnel

The tunnel, measuring approximately 0.7 m in depth and 0.5 m in internal width (average), was constructed using small stones and white silt concretion. Its floor was plastered with gray plaster. The roof of the tunnel was covered with large rectangular plates, primarily made of limestone and BR. The plates averaged 0.56 × 0.78 m in size and 0.12 m in thickness, with maximum dimensions reaching 0.85 × 1 m (Figure 3). Smaller stones were placed between the plates, some positioned directly on the tunnel roof, while others were arranged in a gable-like form, possibly serving as manholes or inspection entrances (Figure 3b).

In the eastern part of the excavation, the tunnel diverged into an "excess tunnel" (L30275), measuring approximately 6 m in length and 0.56 m in width, with side walls about 0.7 m in height. This excess tunnel exits in a northeast direction (Figure 3c). The joint between the main tunnel and the excess tunnel was constructed as a single unit, indicating that both features belonged to the same operational phase.

4.1.2. Beachrock Slabs as Parts of Walls and Apparatus

In two rooms (4 and 5, area G6a), a floor made of large BR plates was discovered (Figure 4a). In room 4, the floor dates to the end of the Byzantine period, and in room 5 the floor is dated to the Umayyad period. Beachrocks were also combined in a built winepress (Figure 4b) in area G7c, dated to Umayyad period. It is constructed of treading floor (L37021), and north of it is a working surface (L37034) paved with irregular BR plates (0.4 × 0.6 m average measure), with pair of square collecting vats (L37038, L37037).

4.1.3. Round Milling Stones

Two round milling stones were discovered. The first stone (L38005) was found in Area G7d and measured 0.34 m in diameter and 0.05–0.1 m in thickness. It featured a central hole (0.027 m in diameter) for a stick (Figure 5a). The second stone (L353369), discovered in Area G6a, had a diameter of 0.44 m and a thickness of 0.075–0.09 m. Unlike the first, it lacked a central hole and may have served as a lower millstone (Figure 5b).

4.1.4. Remarkable Square BR Plates

Two notable square BR plates were found in Area G5. The first plate (L34304) measured 0.84 × 0.89 m with a thickness ranging from 0.12 to 0.17 m (Figure 5c). It featured four curved dimples, each measuring 0.08 m in diameter and 0.05 m in depth. The second plate (Figure 5d) exhibited four curved pits with dimensions similar to those of the first plate. The distances between the dimples were consistent and repetitive, suggesting deliberate design.

4.2. Laboratory Analysis

Both the samples obtained from BR artifacts and from in-situ BR outcrops primarily consist of a typical (Table 2) mixture of three end components (Figures 6–8): Glycymeris bivalves (whole and fragmented); sub-rounded, fine detrital, Nile-derived quartz grains; and reworked (well-rounded, sand to granule-sized) local aeolianite interclasts. The samples show minor, variable presence of fragmented ceramic remains and unidentified biogenic remains (Figures 7 and 8). Many samples consist of gravelly molluscan coquina [22]. The micro-morphological structures exhibit similarities to the cementation processes of inter-

tidal BR formed in the eastern Mediterranean marine environment during the second half of the Holocene [5,8,21,22,24]. These features include rims of micritic (<10 μm thick) calcite surrounding clasts and extended aragonite crystals growing up to ~10–200 μm in length into intergranular pore spaces (Figure 6a). The pore space in the analyzed samples ranges 5–12%.

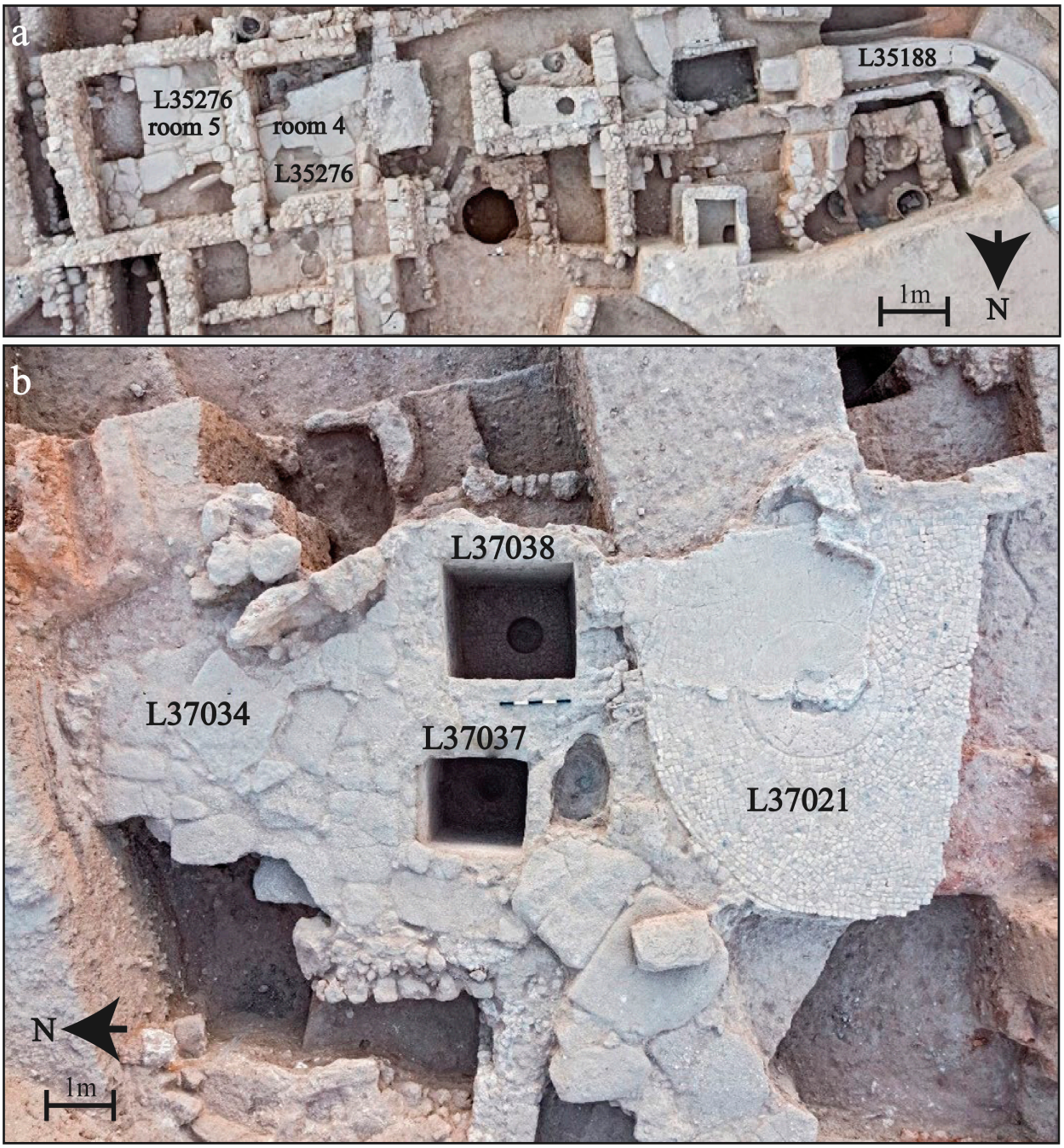

Figure 4. Beachrock usage in architecture within the industrial compound at Tel Yavne. See Figure 2 for the locations of the excavation areas: (**a**) Beachrock plates covering drainage tunnel (L35188) and forming the floors of rooms 4 and 5 in Area G6a. (**b**) Working surface made of beachrock plates (L37034) in a built winepress in Area G7c (photos: A. Peretz). Courtesy of the IAA.

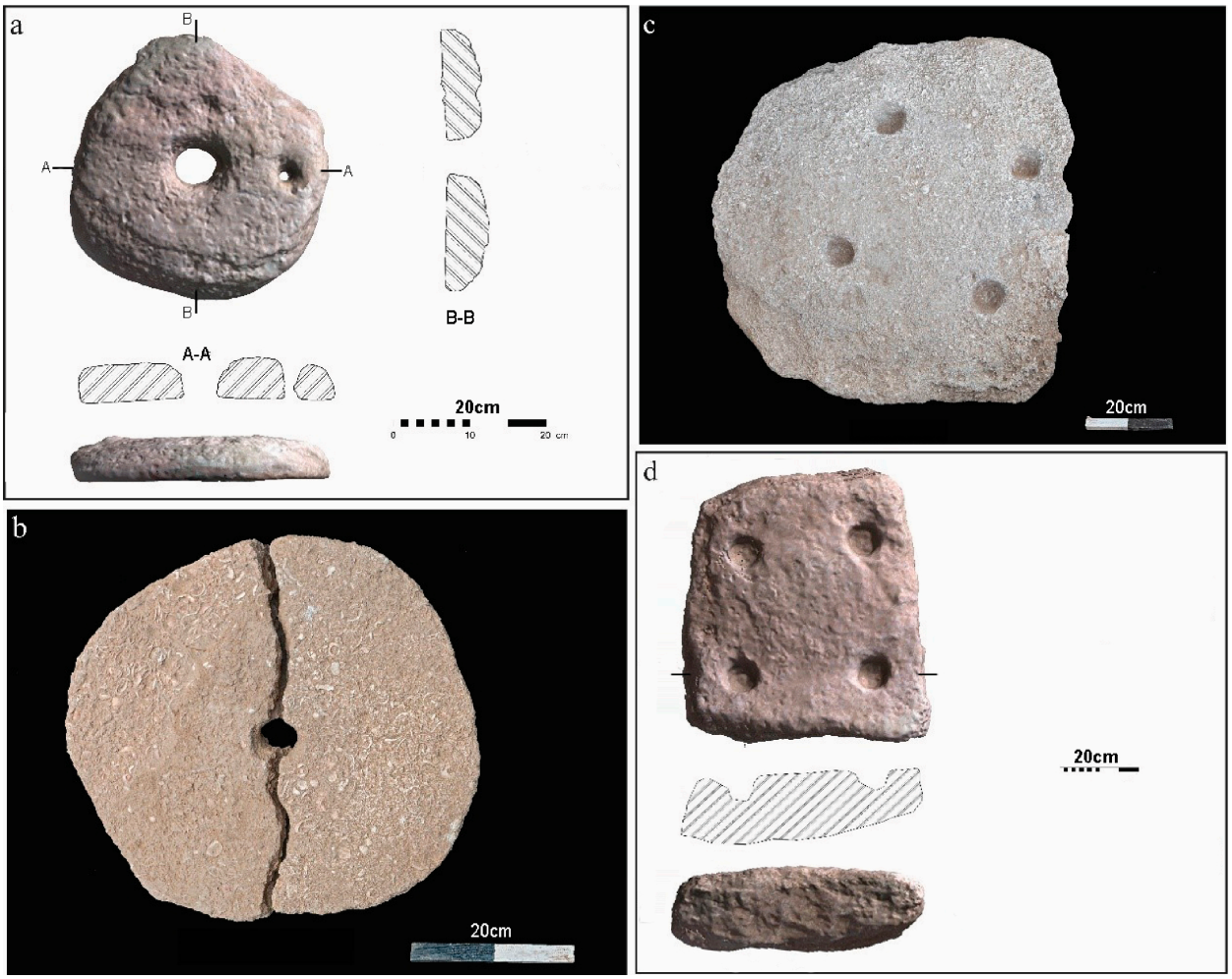

Figure 5. Artifacts made of beachrock from Area G6a and Area G5 (see Figure 2 for locations): (**a**) Round millstone (L38005) (3D modeling: K. Sorkin). (**b**) Round millstone (L35369) (photo: A. Peretz). (**c**) Plate with curved dimples (L34304); scale bar: 0.2 m (photo: A. Peretz). (**d**) Plate with curved dimples or devices (L34303) (3D modeling: K. Sorkin). Courtesy of the IAA.

Table 2. Properties of in-situ beachrock sampled.

Beach	Sample	BR Bed Width (m)	BR Bed Thickness	Composition
Palmachim	PAL-1	3	0.20	Typical
	PAL-2	1	0.15	Many shells
	PAL-3	1	0.15	Many shells
	PAL-4	18	0.15	Typical
	PAL-5	20	0.10	Typical
Ashdod	ASD-1	0.5	0.10	Coquina
	ASD-2	1.5	0.30	Many shells
	ASD-3	3	0.20	Many shells
Ashkelon	ASK-1	55	0.15	Typical
	ASK-2	22	0.20	Coquina

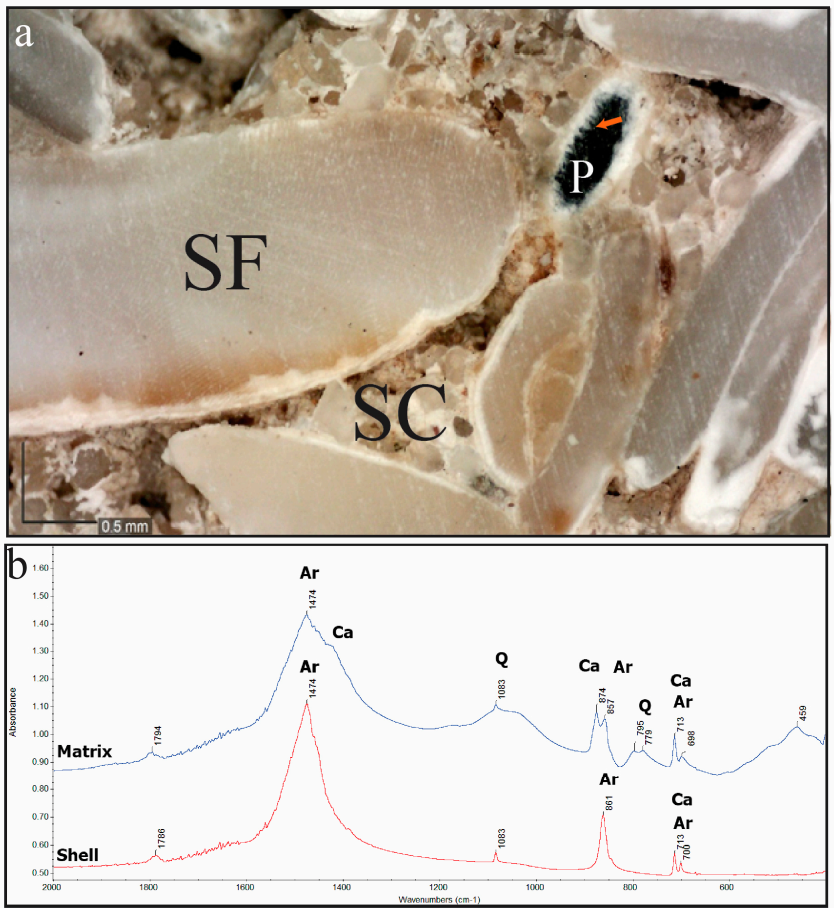

Figure 6. (**a**) Polished surface of beachrock sample from plate covering drainage tunnel under digital microscope (micrograph: Van Zuiden) (SF: shell fragment, SC: siliciclastic quats, P: pore space; the arrow points to cement growing into intergranular pore) and (**b**) FTIR results of the sample (Ar: aragonite, Ca: calcite, Q: quartz). Courtesy of the IAA.

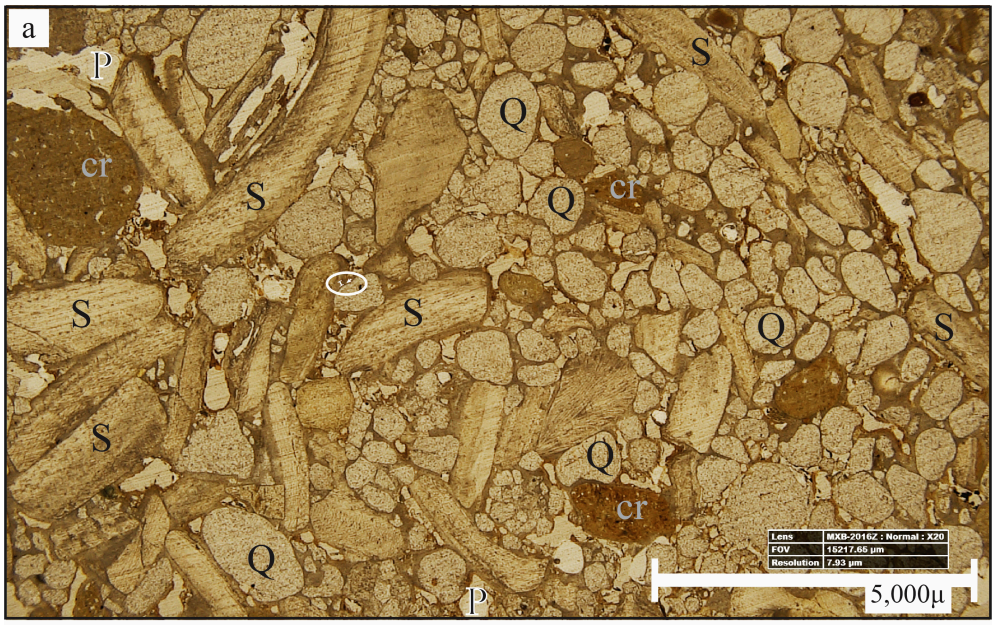

Figure 7. *Cont.*

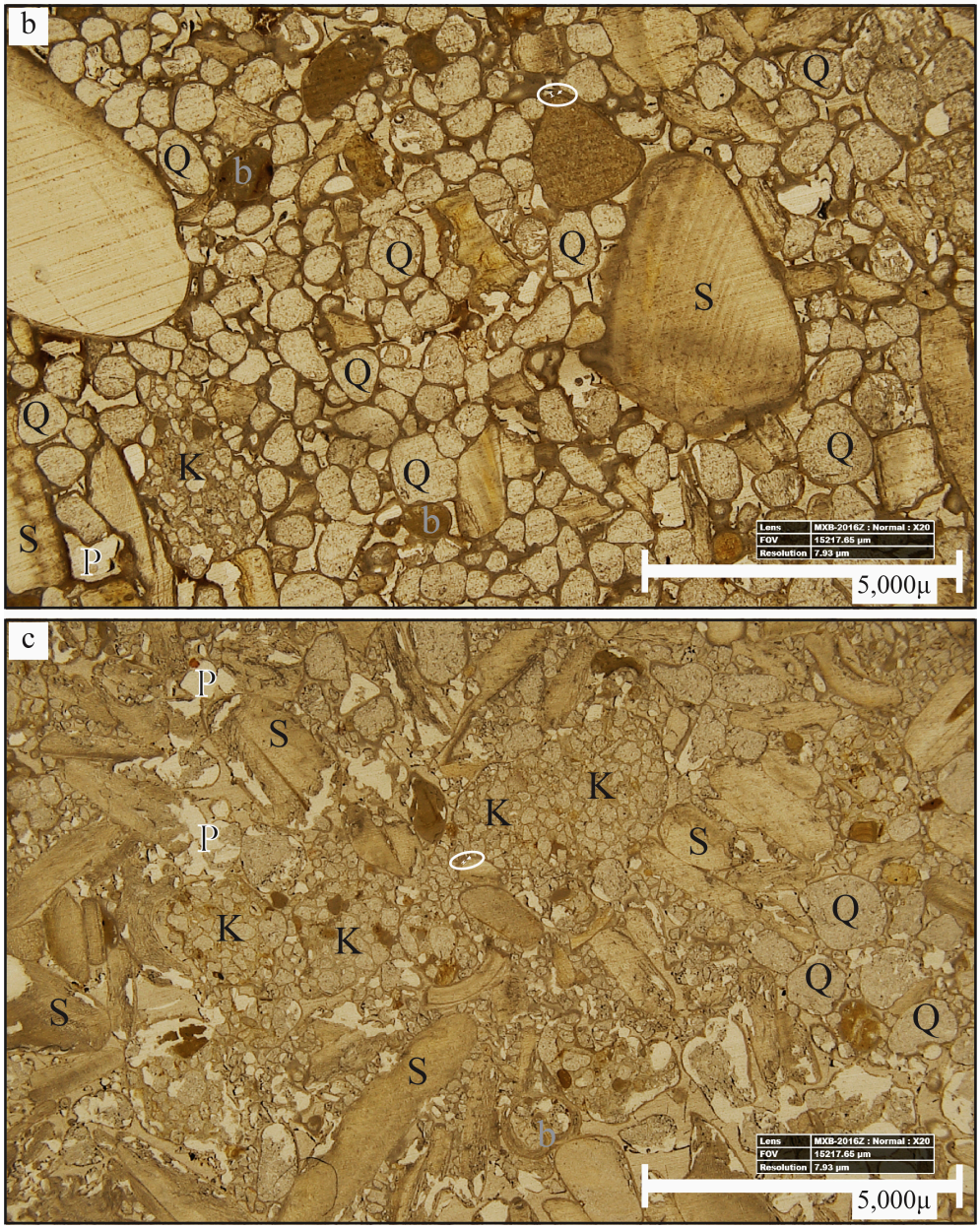

Figure 7. Micrographs of thin sections obtained from in-situ beachrock outcrop samples in southern Israel. All sections were captured under a digital microscope without polarization. Labels: S—Shell fragment; Q—Quartz grain; K—Kurkar fragment; P—Intergranular space; cr—Ceramic fragment; b—Undefined bioclast. (Micrographs: Cohen, M.) (**a**) Tel Ashkelon Beach: Moderately well-sorted beachrock composed primarily of elongated shell fragments. Also includes well-rounded quartz sand, ceramic fragments, and various undefined bioclasts. Cementation consists of microcrystalline calcite and acicular aragonite carbonate cements. Estimated porosity: ~5%. (**b**) Tel Ashkelon Beach: Well-sorted beachrock composed primarily of rounded quartz sand. Also contains shell fragments, well-rounded sand- to granule-sized aeolianite fragments, ceramic fragments, and finer undefined bioclasts. Cementation consists of microcrystalline calcite and acicular aragonite carbonate cements. Estimated porosity: ~5%; (**c**) Tel Yavne Yam Beach (south of Palmachim): Moderately sorted BR composed mainly of shell parts and also contains rounded sand- to granule-size aeolianite fragments and quartz sand and various finer undefined bioclasts cemented with microcrystalline calcite and acicular aragonite carbonate cements. The porosity level estimation is ~5%.

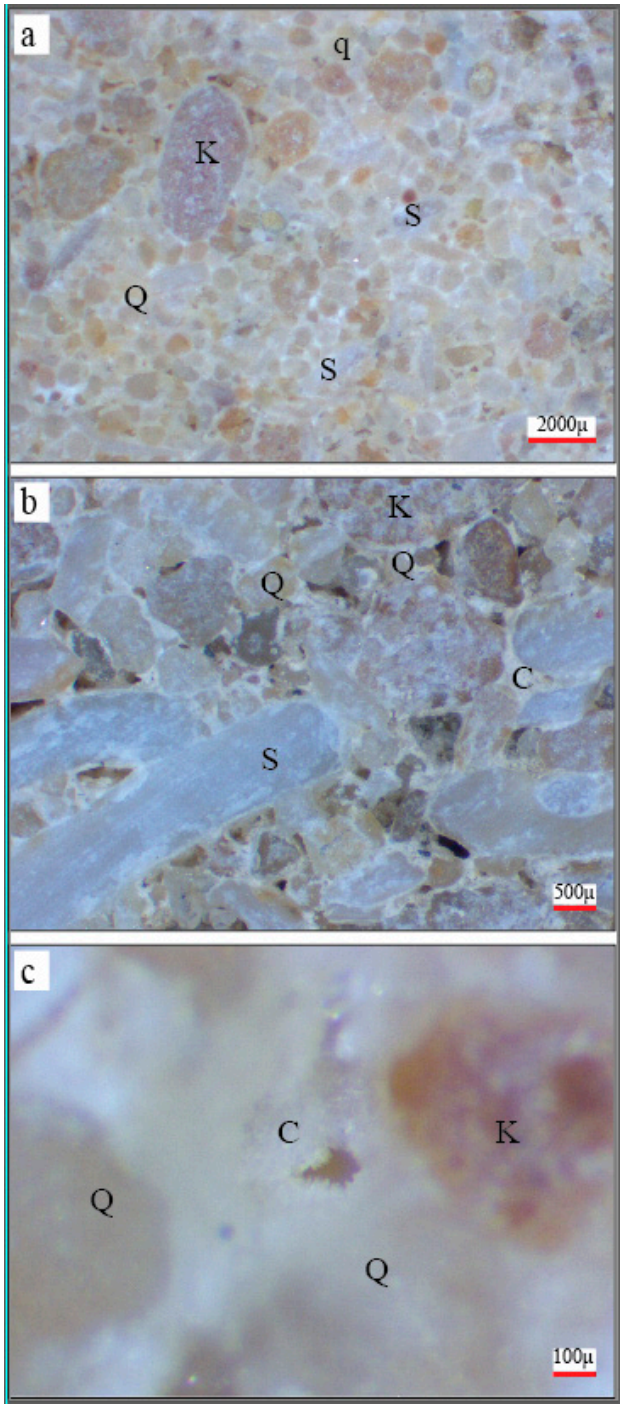

Figure 8. Micrographs of sections obtained from in-situ beachrock outcrop samples from Palmachim Beach: (**a**) moderately well-sorted beachrock composed of mixture of well-rounded quartz and fragmented kurkar sand and shell fragments (scale is 2000µ, PAL-4 in Table 2); (**b**) moderately sorted BR composed primarily of shell fragments and also contains well-rounded quartz sand and sand- to granule-sized rounded kurkar (PAL-3 in Table 2); (**c**) view of cements at intergranular pore between clasts (scale is 100µ PAL-4 in Table 2). Notes: S: shell fragment, Q: siliciclastic quartz grain, K: kurkar fragment, C: cement.

FTIR analysis enabled the identification of the main minerals present in a BR sample from a roofing plate in the tunnel (Figure 6b). These include aragonite, calcite, and quartz. Further FTIR analysis of a subsample taken from a shell fragment within a BR plate show that aragonite is the primary mineral in its composition.

The XRD analysis shows the relative composition (Supplementary Materials—Table S1) of quartz (average 60.5%, ranges 32–89%), aragonite (average 28.73%, ranges 3–58), and Mg Calcite (average 18.65%, 5.7–87) in samples from the Yavne excavation, Palmachim Beach, and Ashdod Beach.

5. Discussion

Previous studies have demonstrated that BR was exploited as a raw material in antiquity and had been used to produce querns at sites along the coastal plain of Israel and that BR was chosen due to geo-economic considerations. These include the abundance of the material, the ease of extraction, the proximity of natural deposits to usage locations, and its mechanical properties such as hardness, coarse matrix, and durability against erosion.

This study presents BR finds from the excavations at Yavne, focusing on the usage of this material. Analyses of the clastic and mineralogical composition of BR samples obtained from artifacts made of BR and from natural BR outcrops show that the clastic composition of in-situ BR outcrops vary between nearby locations but remains generally consistent along the southern coast, consisting primarily of shell fragments, quartz grains, and fragmented rocks. Local variations in particle composition are influenced by factors such as morphodynamics, bathymetry, bedrock identity, backshore morphology, lithostratigraphy, and proximity to stream mouths.

All samples included similar carbonate cement forms typical of Holocene BR outcrops [10,21–24]. The relative contribution of cement to the total weight of the carbonate fraction of the sample is small compared to the contribution of the shell fragments. Thus, the overall mineral composition of the samples corresponds to the clastic compositions. Since the clastic composition varies strongly, and each site includes various cases, determining the exact original location demands further analysis for better indication. It can be carefully suggested that near Yavne Yam the beach material and the BR show stronger presence of kurkar fragments, although the strong presence of shells and fragmented shells is the most distinctive for the southern coast of Israel.

BR samples from the Yavne apparatus and natural outcrops are compact and well-cemented. The mechanical properties of BR—its consolidated structure, hardness, and durability against liquid percolation—are attributable to its naturally homogeneous and well-sorted composition of quartz grains, shells, and fragmented rocks, as well as the characteristics of its cementation.

The finds from the Yavne East excavations reveal that BR was utilized on a large scale for various purposes during the Byzantine period. This is the first large-scale archaeological excavation where significant emphasis was placed on studying BR finds. The evidence suggests that BR was quarried from a nearby location and transported to Yavne, approximately 7 km from the coastline. Despite the availability of closer kurkar sandstone outcrops, two explanations are proposed for the preference for BR:

1. Mechanical Properties: BR's natural composition, structure, and consolidation offer superior strength and durability against abrasion compared to local kurkar. These properties made it particularly suitable for construction uses such as roofing and flooring.
2. Ease of Extraction: BR outcrops along the Mediterranean coast are subject to intense erosion in dynamic environments characterized by strong waves, tides, and currents. These forces create distinctive erosion patterns, such as cracks, stair-like morphologies, and shelves, which facilitate the detachment of large, flat plates. Additionally, the actions of waves and currents often result in BR plates breaking off and accumulating near the backshore, making collection and transport easier.

The typical thickness of BR beds (0.10–0.20 m) aligns with the dimensions of plates found in Yavne, which were likely used without extensive shaping. The slabs were arranged as polygonal mosaics in their natural forms, requiring minimal chiseling. This contrasts with the labor-intensive process of quarrying large chunks from kurkar outcrops and shaping them into usable plates. Instead, BR plates could be collected directly from the beach and transported to the site, potentially using beasts of burden from the nearest beach—north of Ashdod. Another potential source is the beaches near Yavne Yam, with transportation via the route following Nahal Soreq. It is less likely that BRs were collected from the beaches near the Nahal Soreq outlet because river mouths along the Mediterranean coast of Israel are heavily deposited with Nilotic sand most of the year [78]. An additional provenance possibility is the Ashkelon environment, with BR plates arriving to Yavne Yam as salable ballast in small boats.

6. Conclusions

This study presents and discusses the BR finds from the Tel Yavne site, including their sedimentological characterization. The findings demonstrate that BR, quarried from natural deposits along the coastline opposite Tel Yavne, served as a valuable natural resource in antiquity. The use of BR by the constructors of the Byzantine–Early Islamic industrial compound at Yavne was likely driven by its practical and geo-economic advantages. These advantages included its mechanical properties, ease of extraction, and proximity to the site, making it a preferred material for specific construction purposes. The BR brought to Yavne were probably collected from concentrations of BR plates, detached from the main BR exposure band (due to wave erosion) and dropped and settled near the waterfront or thrown by waves to the backshore. Beachrock occurrences are currently observed along a significant part of the Israeli shoreline. The archeological evidence of BR finds in many sites in Israel indicates similar situations during the Byzantine and early Islamic periods.

Supplementary Materials: The following supporting information can be downloaded at: https://www.mdpi.com/article/10.3390/jmse13020240/s1, Table S1: XRD results of BR samples from natural outcrops at the southern Mediterranean coast of Israel and form Yavne excavation artifacts.

Author Contributions: Conceptualization, A.B. and E.H.; methodology, A.B., E.H. and Y.A.; validation, A.B. and E.H.; formal analysis, A.B. and Y.A., investigation, A.B., E.H., Y.A., E.G., R.B. and D.Z.; resources, A.B., E.H., Y.A., E.G., R.B. and D.Z.; data curation, A.B., E.H. and Y.A.; writing—original draft preparation, A.B.; writing—review and editing, A.B., E.H., Y.A., E.G., R.B. and D.Z.; visualization, A.B., Y.A., E.G. and D.Z.; supervision, D.Z., R.B. and E.H. All authors have read and agreed to the published version of the manuscript.

Funding: This research received no external funding.

Institutional Review Board Statement: Not applicable.

Informed Consent Statement: Not applicable.

Data Availability Statement: All the relevant details are presented in the article and in the Supplementary Materials. Any questions will be welcome, addressed via the corresponding authoress.

Acknowledgments: The authors are grateful to Reuven Bar for assistance in sample collection from the beach; Chen Elimelech for sampling in Yavne; Aliza Van Zuiden and Nimrod Wieler for sample preparations and measurements; Asasf Peretz for photography and image processing of the areas and the finds in the studio; Kaya Sorkin for the 3D scanning of BR finds; Yuliya Gumenny for preparation of the excavation plans for the paper; Tamar Harpak for all the logistic attention in providing access to the finds for the research; J.J Gottlieb for thin-section preparation; Maayan Cohen and Deborah Cvikel for digital microscope images; and Nimer Taha for XRD analysis.

Conflicts of Interest: The authors declare no conflicts of interest.

Abbreviations

The following abbreviations are used in this manuscript:

BR	Beachrock
BD	Beach deposits of the last interglacial maximum (MIS 5e)
BP	Before present
NYD	Not yet determined
IAA	Israel Antiquities Authority

References

1. Komar, P.D. *Beach Processes and Sedimentation*; Prentice-Hall, Inc.: Englewood Cliffs, NJ, USA, 1976; p. 429.
2. Danjo, T.; Kawasaki, S. Characteristics of Beachrocks: A Review. *Geotech. Geol. Eng.* **2014**, *32*, 215–246. [CrossRef]
3. Neumeier, U. Experimental Modelling of Beachrock Cementation under Microbial Influence. *Sediment. Geol.* **1999**, *126*, 35–46. [CrossRef]
4. Friedman, G.M. Beachrocks record Holocene events, including natural disasters. *Carbonates Evaporites* **2011**, *26*, 97–109. [CrossRef]
5. Mauz, B.; Vacchi, M.; Green, A.; Hoffmann, G.; Cooper, A. Beachrock: A Tool for Reconstructing Relative Sea Level in the Far-Field. *Mar. Geol.* **2015**, *362*, 1–16. [CrossRef]
6. Karkani, A.; Evelpidou, N.; Vacchi, M.; Morhange, C.; Tsukamoto, S.; Frechend, M.; Maroukiana, H. Tracking shoreline evolution in central Cyclades (Greece) using beachrocks. *Mar. Geol.* **2017**, *388*, 25–37. [CrossRef]
7. Karkani, A.; Evelpidou, N.; Saitis, G.; Tsanakas, K.; Drinia, H.; Vassilakis, E.; Karymbalis, E.; Batzakis, D.V. Coastal Evolution and Relative Sea Level Changes at Psatha (Alkyonides Bay, Greece). *J. Mar. Sci. Eng.* **2023**, *11*, 199. [CrossRef]
8. Polidorou, M.; Saitis, G.; Evelpidou, N. Beachrock developments as an indicator of palaeogegraphic evolution, the case of Akrotiri Peninsula, Cyprus. *Z. Fuur Geomorphol.* **2021**, *63*, 3–17. [CrossRef]
9. Vousdoukas, M.I.; Velegrakis, A.F.; Plomaritis, T.A. Beachrock Occurrence, Characteristics, Formation Mechanisms and Impacts. *Earth Sci. Rev.* **2007**, *85*, 23–46. [CrossRef]
10. Bar, A.; Zviely, D.; Roskin, J.; Galili, E.; Porat, N.; Bookman, R. Beachrock: A chronological benchmark for Late Holocene build-up on the coast of Israel. *Geomorphology* **2024**, *465*, 109408. [CrossRef]
11. McCutcheon, J.; Nothdurft, L.D.; Webb, G.E.; Paterson, D.; Southam, G. Beachrock formation via microbial dissolution and re-precipitation of carbonate minerals. *Mar. Geol.* **2016**, *382*, 122–135. [CrossRef]
12. Malta, J.V.; Castro, J.W.A.; Cabral, C.L.; Fernandes, D.; Cawthra, H.C. Genesis and age of beachrock on the Rio de Janeiro coastline, Southeast–Brazil. *Mar. Geol.* **2021**, *442*, 106649–106661. [CrossRef]
13. García-Hidalgo, J.F.; Elorza, J. Facies model, cementation and sedimentary evolution of a 20th-centurybeach and beachrock: The Gorrondatxe wave and tidal coastal system (NE Spain). *Sediment. Geol.* **2022**, *442*, 106291. [CrossRef]
14. Cooper, J.A.G.; Green, A.N.; Vital, H.; Lima-Filho, F.P. Geomorphology and Clast Assemblages of Intertidal Beachrock: Implications for Submerged Shoreline Preservation. *Geomorphology* **2019**, *343*, 106–118. [CrossRef]
15. Alexandrakis, C.; Ghionis, G.; Poulos, S.S. The effect of beachrock formation on the morphological evolution of a beach, the case study of an eastern Mediterranean beach: Ammoudara, Greece. *J. Coast. Res.* **2013**, *69*, 47–59. [CrossRef]
16. Bar, A.; Bookman, R.; Galili, E.; Zviely, D. Beachrock Morphology along the Mediterranean Coast of Israel: Typological Classification of Erosion Features. *J. Mar. Sci. Eng.* **2022**, *10*, 1571. [CrossRef]
17. Almagor, G.; Gill, D.; Perath, I. Marine sand resources offshore Israel. Mar. *Georesour. Geotec.* **2000**, *18*, 1–42. [CrossRef]
18. Zviely, D.; Kit, E.; Klein, M. Longshore sand transport estimates along the Mediterranean coast of Israel in the Holocene. *Mar. Geol.* **2007**, *238*, 61–73. [CrossRef]
19. Garzanti, E.; Andò, S.; Padoan, M.; Vezzoli, G.; El Kammar, A. The modern Nile sediment system: Processes and products. *Quat. Sci. Rev.* **2015**, *130*, 9–56. [CrossRef]
20. Schattner, I. *Geomorphology: The Exogene Evolution of the Relief*; Kiryath Sepher Ltd.: Jerusalem, Israel, 1970; p. 372.
21. Almagor, G.; Perath, I. *Mediterranean Coast of Israel, Report GSI/28/2016*, 5th ed.; Geology Survey of Israel: Jerusalem, Israel, 2021; p. 438. (In Hebrew)
22. Gavish, E.; Friedman, G.M. Progressive Diagenesis in Quaternary to Late Tertiary Carbonate Sediments: Sequence and Time Scale. *J. Sediment. Petrol.* **1969**, *39*, 980–1006.
23. Bakler, N.; Amiel, A. Morphology and mineralogy of recent beachrocks along the Mediterranean coast of Israel. In Proceedings of the Israel Geological Society Annual Meeting, Ashqelon, Israel, 1–2 June 1976.
24. Magaritz, M.; Gavish, E.; Bakler, N.; Kafri, U. Carbon and oxygen isotope composition indicators of cementation environment in recent, Holocene, and Pleistocene sediments along the coast of Israel. *J. Sediment. Petrol.* **1979**, *49*, 401–412.
25. Bakler, N.; Neev, D.; Magaritz, M. Late Holocene tectonic movments at Tel Haraz, southern coast of Israel. *Earth Planet. Sci. Lett.* **1985**, *75*, 223–230. [CrossRef]

26. Galili, E.; Zviely, D. Geo-archaeological Markers Reveal Magnitude and Rates of Israeli Coastal Cliff Erosion and Retreat. *J. Coast. Conserv.* **2019**, *23*, 747–758. [CrossRef]
27. Mushkin, A.; Katz, O.; Porat, N. Overestimation of Short-Term Coastal Cliff Retreat Rates in the Eastern Mediterranean Resolved with a Sediment Budget Approach. *Earth Surf. Process. Landf.* **2019**, *44*, 179–190. [CrossRef]
28. Raban, A. The Phoenician Harbour and "Fishing Village" at Atlit. *Eres Isr.* **1996**, *25*, 490–508. (In Hebrew). Available online: https://www.jstor.org/stable/23629674 (accessed on 1 October 2022).
29. Antonioli, F.; Mourtzas, N.; Anzidei, M.; Auriemma, R.; Galili, E.; Kolaiti, E.; Lo Presti, V.; Mastronuzzi, G.; Scicchitano, G.; Spampinato, C.; et al. Millstone quarries along the Mediterranean coast: Chronology, morphological variability and relationships with past sea levels. *Quat. Int.* **2017**, *439*, 102–116. [CrossRef]
30. Galili, E.; Zviely, D.; Ronen, A.; Mienis, H.K. Beach Deposits of MIS 5e high Sea Stand as Indicators for Tectonic Stability of the Carmel Coastal Plain, Israel. *Quat. Sci. Rev.* **2007**, *26*, 2544–2557. [CrossRef]
31. Sivan, D.; Sisma-Ventura, G.; Greenbaum, N.; Bialik, O.M.; Williams, F.H.; Tamisiea, M.E.; Rohling, E.J.; Frumkin, A.; Avnaim-Katav, S.; Shtienberg, G.; et al. Eastern Mediterranean Sea Levels through the Last Interglacial from a Coastal-Marine sequence in Northern Israel. *Quat. Sci. Rev.* **2016**, *145*, 204–225. [CrossRef]
32. *The Zifzif Commission Report*; Minister of Housing and Development: Jerusalem, Israel, 1964. (In Hebrew)
33. Emery, K.O.; Neev, D. Mediterranean Beaches of Israel. *Geol. Surv. Bull.* **1960**, *26*, 1–23.
34. Nol, H. Rolling stones: Distribution patterns of marble, basalt and beachrock from Early Medieval Israel. In *Riches Beyound the Horizon-Long–Distance Trade in Eaely Medieval Landscaeps (ca. 6th–12th Centuries)*; Nol, H., Ed.; Post-Medieval Mediterranean Archaeology Series IV; Medieval and BREPOLS Publishers N.V.: Turnhout, Belgium, 2021; pp. 203–235. [CrossRef]
35. Frankel, R. Millstones and grinding stones in the Talmudic literature: Reconsidering according to the archaeological finds. *Cathedra* **2003**, *110*, 43–60.
36. Frankel, R. *Water Mills in Israel*; Open edition books; Publications du Centre Jean Bérard: Naples, Italy, 2007; pp. 215–224.
37. Epstein, C. A Pottery Neolithic site near Tel Qatif. *Isr. Explor. J.* **1984**, *34*, 209–219. Available online: https://www.jstor.org/stable/27925948 (accessed on 12 December 2024).
38. Rowan, Y.M. The Groundstone Assemblages. In *'En Esur ('Ein Asawir): Excavations at a Protohistoric Site in the Coastal Plain of Israel*; Yannai, E., Ariel, D.T., Carmi, I., Grosinger, Z., Horowitz, A., Khalaily, H., Lazar-Shorer, D., Marder, O., Milevski, I., Rowan, Y.M., et al., Eds.; Israel Antiquities Authority Reports; Israel Antiquities Authority: Jerusalem, Israel, 2006; pp. 211–250. [CrossRef]
39. Ebeling, J.R. Groundstone Objects. In *Tel Mor, the Moshe Dothan Excavations, 1959–1960*; Barako, T.J., Ariel, D.T., Brandl, B., Ebeling, J.R., Hirschfeld, N., Maddin, R., Maher, E.F., Martin, M.A.S., Muhly, J.D., Reese, D.S., et al., Eds.; Israel Antiquities Authority Reports; Israel Antiquities Authority: Jerusalem, Israel, 2007; pp. 223–228. Available online: https://www.jstor.org/stable/j.ctt1fzhddh.14 (accessed on 12 December 2024).
40. Sidi, N. The Stone Implements from Gane Tal. *Atiqot* **2021**, *102*, 243–256. Available online: https://www.jstor.org/stable/10.2307/27005180 (accessed on 12 December 2024).
41. Vered, A. Groundstone Tools from Khirbat el-'Umdan, Bet Shemesh. *Atiqot* **2021**, *104*, 19–26. Available online: https://www.jstor.org/stable/10.2307/27054036 (accessed on 12 December 2024).
42. Rosenberg, D. The Groundstone Assemblage. In *The Early Bronze Age Site: Volume II: The Finds*; Golani, A., Ed.; IAA Reports; Israel Antiquities Authority: Jerusalem, Israel, 2022; Volume 70, pp. 135–180. [CrossRef]
43. Neri, Y. Archaeological and Geological Aspects of Beachrock Saddle-Querns Utilization in Antiquity. Master's Thesis, University of Haifa, Haifa, Israel, 1994.
44. Tatcher, A. The Hospitaller Compound: Ballista Balls. In *Akko II the 1991–1998 Excavations: The Early Periods*; Hartal, M., Syon, D., Stern, E., Tatcher, A., Eds.; Israel Antiquities Authority Reports; Israel Antiquities Authority: Jerusalem, Israel, 2016; Volume 60, pp. 127–129.
45. Kletter, R. Early Islamic remains at 'Opher Park', Ramla. *Atikot* **2005**, *49*, 57–99.
46. Tal, O.; Taxel, I. The Site and its Excavation History. In *Ramla (South) an Early Islamic Industrial Site and Remains of Previous Periods*; Tal, O., Taxel, I., Eds.; Sonia and Marco Nadler Institute of Archaeology: Tel Aviv, Israel, 2008; pp. 7–16.
47. Tal, O.; Taxel, I. Subterranean Valuated Chambers. In *Ramla (South) an Early Islamic Industrial Site and Remains of Previous Periods*; Tal, O., Taxel, I., Eds.; Sonia and Marco Nadler Institute of Archaeology: Tel Aviv, Israel, 2008; pp. 111–115.
48. Orendi, A.; Yehuda, E.; Zeischka-Kenzler, A.; Tal, O. Flora in the Latin East: Archaeobotanical Remains from Crusader Arsur. *Tel Aviv* **2023**, *50*, 263–288. [CrossRef]
49. Tal, O.; Taxel, I. The Khirbet al-Aura/Tel Barukh Cemetery. In *Samartian Cemeteries and Tombs in the Central Coastal Plain, Archeology and History of the Samaritan Settlement Outside Samaria (ca. 300–700 CE)*; Tal, O., Taxel, I., Eds.; Ugarit–Buch-und Medienhandel GmbH: Münster, Germany, 2015; pp. 1–138.
50. Bouchenino, A, Rehovot, Weizman Institute of Science. *Hadashot Arkheologiyot Excav. Surv. Isr.* **2007**, *119*. Available online: https://www.hadashot-esi.org.il/report_detail_eng.aspx?id=640&mag_id=112 (accessed on 12 December 2024).
51. Toueg, R.; Arnon, Y.D. Ramla, the Pool of Arches: New evidence for the water inlet into the pool. *Atiqot* **2018**, *93*, 125–161.

52. Vunsh, R.; Tal, O.; Sivan, D. Horbat Ashdod-Yam. *Hadashot Arkheologiyot Excav. Surv. Isr.* **2013**, *12*. Available online: https://www.hadashot-esi.org.il/report_detail_eng.aspx?id=2294&mag_id=120 (accessed on 12 December 2024).
53. Fantalkin, A. Ashdod-Yam on the Israeli Mediterranean Coast: A First Season of Excavations. *Skyllis* **2014**, *14*, 45–57.
54. Abu Hamid, A. Gesher Ha-Ziv. *Hadashot Arkheologiyot Excav. Surv. Isr.* **2021**, *133*. Available online: https://www.hadashot-esi.org.il/report_detail_eng.aspx?id=26005&mag_id=133 (accessed on 12 December 2024).
55. Vunsh, R.; Tal, O.; Sivan, D.; Fischer, M. Yavne-Yam. *Hadashot Arkheologiyot Excav. Surv. Isr.* **2014**, *126*. Available online: https://www.hadashot-esi.org.il/report_detail_eng.aspx?id=7483&mag_id=121 (accessed on 12 December 2024).
56. Taxel, I. Land and Sea: On the Relationships, Similarities, and Differences between Yavne and Yavne-Yam from the Persian to the Beginning of the Crusader Period. In *Yavne and Its Secrets: Collected Papers*; Haddad, E., Nadav-Ziv, L., Seligman, J., Betzer, P., Shadman, A., Tal, O., Tepper, Y., Eds.; The Israel Antiquities Authority: Jerusalem, Israel; Tel Aviv University: Tel Aviv, Israel; Israel Land Authority: Jerusalem, Israel, 2022; pp. 25–55, ISBN 978-965-406-766-9.
57. Gendelman, P. (Israel Antiquities Authority, Jerusalem, Israel). Personal communication, 2022.
58. Toueg, R. (Israel Antiquities Authority, Jerusalem, Israel). Personal communication, 2022.
59. Peretz, I. (Israel Antiquities Authority, Jerusalem, Israel). Personal communication, 2022.
60. Shotten-Hallel, V.; Perelis Grossowicz, L.; Mart, Y.; Boas, A.J. The Hospitaller Compound: A Petrographic Analysis of Its Building Stones. In *Akko III–the 1991–1998 Excavations: The Late Periods. Part I, The Hospitaller Compound*; Stern, E., Syon, D., Eds.; IAA Reports; Israel Antiquities Authority: Jerusalem, Israel, 2023; Volume 72, pp. 83–90. Available online: https://www.jstor.org/stable/jj.10656815.10 (accessed on 12 December 2024).
61. Galili, E.; Langgut, D.; Terral, J.F.; Barazani, O.; Dag, A.; Horwitz, L.K.; Ramirez, I.O.; Rosen, B.; Weinstein-Evron, M.; Chaim, S.; et al. Early production of table olives at a mid-7th millennium BP submerged site off the Carmel coast (Israel). *Sci. Rep.* **2021**, *11*, 2218. [CrossRef] [PubMed]
62. Roskin, J.; Ackermann, O.; Asscher, Y.; Marcus, J.; Wieler, N. The Geomorphology and Sedimentology of the Tel Yavneh Environs, Southern Coastal Plain of Israel, and Its Connection to Ancient Human Settlement. In *Yavne and Its Secrets: Collected Papers*; Haddad, E., Nadav-Ziv, L., Seligman, J., Betzer, P., Shadman, A., Tal, O., Tepper, Y., Eds.; The Israel Antiquities Authority: Jerusalem, Israel; Tel Aviv University: Tel Aviv, Israel; Israel Land Authority: Jerusalem, Israel, 2022; pp. 25–55. ISBN 978-965-406-766-9.
63. Sion, O. Tel Yavne. *Hadashot Arkheologiyot Excav. Surv. Isr.* **2005**, *117*. Available online: https://www.hadashot-esi.org.il/report_detail_eng.aspx?id=222&mag_id=110 (accessed on 12 December 2024). [CrossRef]
64. Fischer, M.; Taxel, I. Ancient Yavneh: Its History and Archaeology. *Tel Aviv* **2007**, *34*, 204–284. [CrossRef]
65. Yannai, E. Yavne. *Hadashot Arkheologiyot Excav. Surv. Isr.* **2014**, *126*. Available online: https://www.hadashot-esi.org.il/report_detail_eng.aspx?id=13677&mag_id=121 (accessed on 12 December 2024). [CrossRef]
66. Feldstein, A.; 'Ad, U. Tel Yavne, Southwestern Slope. *Hadashot Arkheologiyot Excav. Surv. Isr.* **2014**, *126*. Available online: https://www.hadashot-esi.org.il/report_detail_eng.aspx?id=13707&mag_id=121 (accessed on 12 December 2024).
67. Zissu, B.; Baruch, E.; Levy-Reife, A. Tel Yavne. *Hadashot Arkheologiyot Excav. Surv. Isr.* **2015**, *127*. Available online: https://www.hadashot-esi.org.il/report_detail_eng.aspx?id=18757&mag_id=122 (accessed on 12 December 2024). [CrossRef]
68. Taxel, I.; Sivan, D.; Bookman, R.; Roskin, J. An Early Islamic Inter-Settlement Agroecosystem in the Coastal Sand of the Yavneh Dunefield, Israel. *J. Field Archaeol.* **2018**, *43*, 551–569. [CrossRef]
69. Nadav-Ziv, L. Yavne. *Hadashot Arkheologiyot Excav. Surv. Isr.* **2020**, *132*. Available online: https://www.hadashot-esi.org.il/report_detail_eng.aspx?id=25743&mag_id=128 (accessed on 12 December 2024). [CrossRef]
70. Nadav-Ziv, L.; Haddad, E.; Seligman, J.; Varga, D.; Betzer, P. Preliminary Finds from the Extensive Excavations at the Foot of Tel Yavne. In *Yavne and Its Secrets: Collected Papers*; Haddad, E., Nadav-Ziv, L., Seligman, J., Betzer, P., Shadman, A., Tal, O., Tepper, Y., Eds.; The Israel Antiquities Authority: Jerusalem, Israel; Tel Aviv University: Jerusalem, Israel; Israel Land Authority: Jerusalem, Israel, 2022; pp. 19–55, ISBN 978-965-406-766-9.
71. Seligman, J.; Haddad, E.; Nadav-Ziv, L. Yavne and the industrial production of Gaza and Ashqelon wines. *Levant* **2023**, *56*, 129–152. [CrossRef]
72. Bar, A.; Haddad, E.; Asscher, Y.; Van Zuiden, A.; Elimelech, C.; Bookman, R.; Zviely, D. Beachrock Finds at Yavne-East Excavations: Preliminary Results. In *Yavne and Its Secrets: Collected Papers*; Haddad, E., Nadav-Ziv, L., Seligman, J., Betzer, P., Shadman, A., Tal, O., Tepper, Y., Eds.; The Israel Antiquities Authority: Jerusalem, Israel; Tel Aviv University: Tel Aviv, Israel; Israel Land Authority: Jerusalem, Israel, 2022; pp. 185–201, ISBN 978-965-406-7660. (In Hebrew)
73. Miller, W.R.; Mason, T.R. Erosional features of coastal beachrock and aeolianite outcrops in Natal and Zululand, South Africa. *J. Coast. Res.* **1994**, *10*, 374–394.
74. Tucker, M.E. *Sedimentary Rocks in the Field: A Practical Guide*, 4th ed.; Wiley-Blackwell: Durham, UK, 2004; p. 304.
75. Tucker, M.E. *Sedimentary Petrology: An Introduction to the Origin of Sedimentary Rocks*, 3rd ed.; Blackwell: Malden, MA, USA, 2001; p. 262.

76. FTIR Library of the Kimmel Center for Archaeological Science. Available online: http://www.weizmann.ac.il/kimmel-arch/infraredspectra-library (accessed on 27 December 2024).
77. Hubbard, C.R.; Snyder, R.L. RIR—Measurement and use in quantitative XRD. *Powder Diffract.* **1988**, *3*, 74–77. [CrossRef]
78. Lichter, M.; Zviely, D.; Klein, M. Morphological patterns of southeastern Mediterranean river mouths: The topographic setting of the beach as a forcing factor. *Geomorphology* **2010**, *123*, 1–12. [CrossRef]

Disclaimer/Publisher's Note: The statements, opinions and data contained in all publications are solely those of the individual author(s) and contributor(s) and not of MDPI and/or the editor(s). MDPI and/or the editor(s) disclaim responsibility for any injury to people or property resulting from any ideas, methods, instructions or products referred to in the content.